Electric Power Systems Research 148 (2017) 230–236

Contents lists available at ScienceDirect

Electric Power Systems Research

journal homepage: www.elsevier.com/locate/epsr

Efficient relaxations for joint chance constrained AC optimal power flow

Kyri Baker[a,*], Bridget Toomey[b]

[a] National Renewable Energy Laboratory, Golden, CO 80401, United States
[b] Alteryx Inc., Broomfield, CO 80021, United States

ARTICLE INFO

Article history:
Received 5 January 2017
Received in revised form 29 March 2017
Accepted 1 April 2017

Keywords:
Chance constraints
Renewable integration
Voltage regulation
Distribution grids
Boole's inequality

ABSTRACT

Evolving power systems with increasing levels of stochasticity call for a need to solve optimal power flow problems with large quantities of random variables. Weather forecasts, electricity prices, and shifting load patterns introduce higher levels of uncertainty and can yield optimization problems that are difficult to solve in an efficient manner. Solution methods for single chance constraints in optimal power flow problems have been considered in the literature, ensuring single constraints are satisfied with a prescribed probability; however, joint chance constraints, ensuring multiple constraints are simultaneously satisfied, have predominantly been solved via scenario-based approaches or by utilizing Boole's inequality as an upper bound. In this paper, joint chance constraints are used to solve an AC optimal power flow problem while preventing overvoltages in distribution grids under high penetrations of photovoltaic systems. A tighter version of Boole's inequality is derived and used to provide a new upper bound on the joint chance constraint, and simulation results are shown demonstrating the benefit of the proposed upper bound. The new framework allows for a less conservative and more computationally efficient solution to considering joint chance constraints, specifically regarding preventing overvoltages.

1. Introduction

Increasing penetrations of intermittent energy sources in the electric power grid, evolving faster than the corresponding infrastructure, can increase the probability that line congestions may occur, and that voltages may lay outside of desired limits. Rather than considering this randomness as a deterministic input or representing the uncertainty via computationally prohibitive scenario-based approaches, we solve a joint chance constraint problem which prevents overvoltages in the grid with a certain probability. Single chance constraints, which ensure that a single constraint is satisfied with a prescribed probability, have been considered in a variety of power systems applications, many addressing the problems of line congestions [1,2], voltage regulation [3,4], unit commitment [5,6], transmission expansion planning [7], and energy storage sizing [8]. These works constrain the individual probability of constraint violations independently; however, considering these constraints separately neglects to explicitly consider simultaneous violation conditions in the *overall* system. For example, in the single chance constraint approach, it may be independently guaranteed that the voltage at each node is under its maximum with a high probability, but this could result in a situation where multiple nodes simultaneously have overvoltage conditions. Thus, perhaps a more relevant constraint to consider is restricting the probability of *all* voltages, line flows, states of charge, etc. being within prescribed limits throughout the system.

Joint chance constraints, which ensure multiple constraints are *simultaneously* satisfied with a given probability, have been considered in [9] for the $N-1$ security problem, and the joint chance constraint problem was solved by utilizing a sample-based scenario approach. In [10], both single and joint chance constraints were considered to mitigate line congestions, and a Monte-Carlo based approach was developed to estimate the joint probability. Due to the difficulty in reformulating joint chance constraints into deterministic ones that can be utilized in an optimization problem, Boole's inequality [11] is a popular choice to provide an upper bound on the original chance constraint [12,13], separating the joint chance constraint $P(g_1(x,\delta)\leq 0,\ \ldots,\ g_n(x,\delta)\leq 0)\leq 1-\epsilon$, where x is a vector of decision variables, δ is a random parameter, and ϵ is the maximum constraint violation probability, into single chance constraints $P(g_1(x,\delta)\leq 0)\leq 1-\epsilon_1 \cdots P(g_n(x,\delta)\leq 0)\leq 1-\epsilon_n$ for $i=1,\ldots,n$, where $\sum_{i=1}^{n}\epsilon_i \leq \epsilon$. A common choice for ϵ_i is usually ϵ/n [12,13]; however, this parameter can also be optimized

* Corresponding author.
E-mail addresses: kyri.baker@nrel.gov (K. Baker), btoomey@alteryx.com (B. Toomey).

http://dx.doi.org/10.1016/j.epsr.2017.04.001
0378-7796/

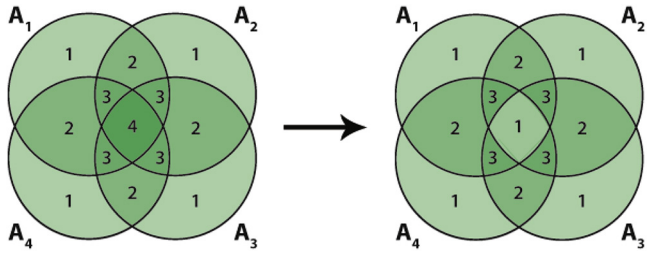

Fig. 1. Illustrative example: When finding an upper bound on the union of events A_1 through A_4, Boole's inequality (left) tends to over-count the intersection of the events (as indicated by the 4), resulting in a loose upper bound. Improved bounds are sought by subtracting the intersection of all events (right), thus counting the intersection only once.

[14]. In [15] a Monte Carlo method is used to solve a sequence of convex optimization problems and compute the joint chance constraint directly; however, it is computationally slow and can only handle relatively small problems. Ambiguous joint chance constraints were studied in [16,17], in which the random parameters are assumed to belong to a so-called ambiguity set. In addition, distributionally robust joint chance constraints are studied in [18] using semidefinite programming based approximations, where the tightness of the approximation is tuned via a sequential convex optimization algorithm.

Our approach requires no parameter tuning, or other computationally burdensome techniques such as including ϵ as an optimization variable and performing further approximations to convexify the problem. Instead, the benefits of utilizing Boole's inequality are enhanced by a fast yet effective method that tightens the chance constraint reformulations in a simple and straightforward way. In addition, by exploiting the structure of the voltage regulation problem; i.e., assuming the probability that the system is operating within normal voltage regions is high, the improved bound decreases the cost of the otherwise overly conservative nature of using Boole-based inequalities. It is shown that the new upper bound is tighter than or equal to Boole's inequality, and intuitively amounts to using a bound on the excess probabilities of the intersection of all events using Fréchet's inequality, or estimating this intersection with a small number of samples, which Boole's inequality overestimates (see Fig. 1 for a four event example).

Finally, by utilizing a linearization of the AC power flows in a distribution network, the chance-constrained voltage regulation problem is solved to address the relevant problem of overvoltages under high penetrations of distributed generation (photovoltaic systems). Simulation results are performed using a modified IEEE-37 node test feeder with community PV systems, and the new bound is compared with a deterministic formulation and the traditional Boole's inequality used in joint chance constraint reformulations. The contributions of this paper are threefold: Firstly, to the best of the authors' knowledge, we present the first joint chance constrained optimal power flow formulation for voltage regulation in distribution grids. Secondly, we present a computationally efficient, simple improvement over a technique that is commonly used to handle joint chance constraints with a tighter upper bound. Lastly, we not only show in simulation the improvement given by the new technique, but we formally prove the tightness of the new bound.

2. Joint chance constraint relaxation

The joint chance constraint considered here requires the probability of all voltages in the system to be under than the maximum voltage limit with a probability greater than or equal to $1-\epsilon$:

$$P(g_1(x,\delta)<0,\ldots,g_n(x,\delta)<0)\geq 1-\epsilon \tag{1}$$

where $g_1(x,\delta)<0,\ldots,g_n(x,\delta)<0$ constrain the voltage magnitude at each bus i, V_i, to be less than to the maximum voltage magnitude $\bar{V}$, x is a vector of decision variables, δ is a jointly distributed Gaussian random vector with mean μ and positive definite covariance matrix Σ, and $\epsilon\in(0,0.5]$. In this case, the vector x represents the voltage magnitudes as well as the controllable amount of curtailed power from each PV system and δ contains the forecasting errors of solar irradiance. In the following analysis, denote event A_i as the event that $g_i(x,\delta)<0$; i.e., that the voltage magnitude at bus i is under the maximum allowable voltage $\bar{V}$.

2.1. Improved Boole's inequality

Considering each constraint i as an event B_i, the joint chance constraint can be written as the intersection of events $P(B_1\cap B_2\cap\cdots\cap B_n)$. Using complementarity, $P(B_1\cap B_2\cap\cdots\cap B_n)=1-P(B_1^c\cup B_2^c\cup\cdots\cup B_n^c)$. For brevity, define event B_i^c as A_i for each i. Boole's inequality states that

$$P\left(\bigcup_{i=1}^{n}A_i\right)\leq P(A_1)+P(A_2)+\cdots+P(A_n) \tag{2}$$

for events A_i, where $i=1,\ldots,n$. However, the sum of individual probabilities is a conservative upper bound for the union; for example, as seen in Fig. 1, the intersection of events is needlessly accounted for multiple times, making the bound defined by Boole's a conservative one. Specifically with regards to the voltage regulation problem, $P(A_1)$, $P(A_2)$, …, $P(A_n)$ refer to the individual probabilities of the voltage at bus $i=1,\ldots,n$ being greater than or equal to $\bar{V}$.

In this paper, we improve the above inequality by providing a new bound that is equal to or tighter than (2). First, consider the following:

$$P\left(\bigcup_{i=1}^{n}A_i\right)\leq P(A_1)+P(A_2)+\cdots+P(A_n)-P(A_1\cap A_2\cap\cdots\cap A_n) \tag{3}$$

Which subtracts the intersection of all events. It is clear that $P(A_1\cap A_2\cap\cdots\cap A_n)\geq 0$, and subtracting this from the sum of the individual probabilities does not remove any portion of the feasible region of the original union, which will be shown later. Thus, we propose (3) as an equal or tighter bound on the union than (2). Further, considering the fact that if this intersection is nonzero, it will be repeated n times, with $n-1$ of those instances being redundant. Thus, we can extend (3) to the following:

$$P\left(\bigcup_{i=1}^{n}A_i\right)\leq P(A_1)+P(A_2)+\cdots +P(A_n)-(n-1)P(A_1\cap A_2\cap\cdots\cap A_n) \tag{4}$$

If this intersection cannot be computed, by using Fréchet's inequality, we can provide an alternate upper bound:

$$P\left(\bigcup_{i=1}^{n}A_i\right)\leq P(A_1)+P(A_2)+\cdots +P(A_n)-(n-1)[P(A_1)+\cdots+P(A_n)-(n-1)]_+ \tag{5}$$

where $[\cdot]_+$ denotes $max(0,\cdot)$.

Proposition 1. *The bounds provided by (4) and (5) provide a valid upper bound that is equal to or tighter than (2).*

Proof. First, we prove by induction that the following inequality holds for any $n=2$ (for $n=1$, the joint constraint becomes a single chance constraint):

$$P(A_1\cup A_2)\leq P(A_1)+P(A_2)-(n-1)P(A_1\cap A_2) \tag{6}$$

By definition, $P(A_1 \cup A_2) = P(A_1) + P(A_2) - P(A_1 \cap A_2)$; thus, the base case holds. Now, assume that case n holds true:

$$P\left(\bigcup_{i=1}^{n} A_i\right) \leq \sum_{i=1}^{n} P(A_i) - (n-1)P\left(\bigcap_{i=1}^{n} A_i\right)$$

we wish to prove that the inequality still holds for $n+1$; that is

$$P\left(\bigcup_{i=1}^{n+1} A_i\right) \leq \sum_{i=1}^{n+1} P(A_i) - nP\left(\bigcap_{i=1}^{n+1} A_i\right)$$

By the base case,

$$P\left(\bigcup_{i=1}^{n+1} A_i\right) \leq \left(P\left(\bigcup_{i=1}^{n} A_i\right) + P(A_{n+1})\right) - P\left(\bigcap_{i=1}^{n} A_i \cap A_{n+1}\right) \tag{7}$$

But

$$\bigcap_{i=1}^{n+1} A_i \subseteq \left(\bigcap_{i=1}^{n} A_i\right) \cap A_{n+1}$$

and thus

$$P\left(\bigcap_{i=1}^{n+1} A_i\right) \leq P\left(\left(\bigcap_{i=1}^{n} A_i\right) \cap A_{n+1}\right)$$

which, by the inductive hypothesis, yields the upper bound

$$P\left(\bigcap_{i=1}^{n+1} A_i\right) leqP\left(\bigcap_{i=1}^{n} A_i\right) + P(A_{n+1}) - P\left(\bigcap_{i=1}^{n+1} A_i\right)$$

$$\leq \sum_{i=1}^{n} P(A_i) - (n-1)P\left(\bigcap_{i=1}^{n} A_i\right) + P(A_{n+1}) - P\left(\bigcap_{i=1}^{n+1} A_i\right)$$

and because $\cap_{i=1}^{n+1} A_i \subseteq \cap_{i=1}^{n} A_i$, $P(\cap_{i=1}^{n+1} A_i) \leq P(\cap_{i=1}^{n} A_i)$. Therefore,

$$P\left(\bigcap_{i=1}^{n+1} A_i\right) \leq \sum_{i=1}^{n} P(A_i) + P(A_{n+1}) - (n-1)P\left(\bigcap_{i=1}^{n+1} A_i\right)$$

$$-P\left(\bigcap_{i=1}^{n+1} A_i\right) \leq \sum_{i=1}^{n+1} P(A_i) - (n)P\left(\bigcap_{i=1}^{n+1} A_i\right)$$

Lastly, by Freéchet's inequality, we have

$$P\left(\bigcap_{i=1}^{n+1} A_i\right) \leq \sum_{i=1}^{n} P(A_i) + n\left[\sum_{i=1}^{n+1} P(A_i) - n\right]_+$$

and the proof by induction is complete. For (4) and (5) to be equal or tighter upper bounds than (2), it is sufficient to show that

$$\sum_{i=1}^{n} P(A_i) - (n-1)\left[\sum_{i=1}^{n} P(A_i) - (n-1)\right]_+ \leq \sum_{i=1}^{n} P(A_i) \tag{8}$$

Because $n > 1$ and $[\sum_{i=1}^{n} P(A_i) - (n-1)]_+ \geq 0$, it is clear that the left hand side of (8) is always less than or equal to the right hand side. For small $\sum_{i=1}^{n} P(A_i)$ or large n, this bound will likely end up being equivalent to Boole's inequality, because $[\sum_{i=1}^{n} P(A_i) - (n-1)]_+$ is likely to be 0. However, for sensitivity studies, such as identifying under which situations the probability of overvoltage is high, this bound could prove useful. For the application considered in this paper, we will utilize the bound (4) which directly considers the intersection.□

2.2. Reformulating the joint chance constraints

Consider the original joint chance constraint and its complement:

$$P(g_1(x,\delta) < 0 \cap \cdots \cap g_n(x,\delta) < 0) \Leftrightarrow$$
$$1 - P(g_1(x,\delta) \geq 0 \cup \cdots \cup g_n(x,\delta) \geq 0)$$

The probability of the union of events can thus be written as

$$P(g_1(x,\delta) \geq 0 \cup \cdots \cup g_n(x,\delta) \geq 0) \leq \epsilon$$

Then, the final joint chance constraint reformulation can be written as the following series of single chance constraints $P(g_1(x,\delta) \geq 0) \leq \epsilon_1, P(g_2(x,\delta) \geq 0) \leq \epsilon_2, \ldots, P(g_n(x,\delta) \geq 0) \leq \epsilon_n$, where, according to (4),

$$\sum_{i=1}^{n} \epsilon_i - P(A_1 \cap \cdots \cap A_n) \cdot (n-1) \leq \epsilon. \tag{9}$$

It will be shown in the following section that the intersection $P(A_1 \cap \cdots \cap A_n)$ can be efficiently estimated using a small number of samples.

3. System model and linearization

3.1. Distribution network

Consider a distribution feeder comprising of $N+1$ nodes collected in the set $\mathcal{N} \cup \{0\}$, $\mathcal{N} := \{1, \ldots, N\}$, and lines represented by the set of edges $\mathcal{E} := \{(m,n)\} \subset \mathcal{N} \times \mathcal{N}$. Let $V_n \in \mathbb{C}$ and $I_n \in \mathbb{C}$ denote the phasors for the line-to-ground voltage and the current injected at node $n \in \mathcal{N}$, respectively, and define the N-dimensional complex vectors $\mathbf{v} := [V_1, \ldots, V_N]^{\mathsf{T}} \in \mathbb{C}^N$ and $\mathbf{i} := [I_1, \ldots, I_N]^{\mathsf{T}} \in \mathbb{C}^N$. Node 0 denotes the secondary of the distribution transformer, and it is taken to be the slack bus. Using Ohm's and Kirchhoff's laws, the following linear relationship can be established:

$$\begin{bmatrix} I_0 \\ \mathbf{i} \end{bmatrix} = \underbrace{\begin{bmatrix} y_{00} & \bar{\mathbf{y}}^{\mathsf{T}} \\ \bar{\mathbf{y}} & \mathbf{Y} \end{bmatrix}}_{:=\mathbf{Y}_{\text{net}}} \begin{bmatrix} V_0 \\ \mathbf{v} \end{bmatrix} \tag{10}$$

where the admittance matrix $\mathbf{Y}_{\text{net}} \in \mathbb{C}^{N+1 \times N+1}$ is formed based on the system topology and the π-equivalent circuit of the distribution lines, and is partitioned in sub-matrices with the following dimensions: $\mathbf{Y} \in \mathbb{C}^{N \times N}$, $\bar{\mathbf{y}} \in \mathbb{C}^{N \times 1}$, and $y_{00} \in \mathbb{C}$. The voltage at the slack bus is defined as $V_0 = \rho_0 e^{j\theta_0}$, with ρ_0 denoting the voltage magnitude at the secondary of the step-down transformer. Lastly, $P_{\ell,n}$ and $Q_{\ell,n}$ denote the real and reactive demands at node $n \in \mathcal{N}$, and define the vectors $\mathbf{p}_\ell := [P_{\ell,1}, \ldots, P_{\ell,N}]^{\mathsf{T}}$ and $\mathbf{q}_\ell := [Q_{\ell,1}, \ldots, Q_{\ell,N}]^{\mathsf{T}}$; if no load is present at node $n \in \mathcal{N}$, then $P_{\ell,n} = Q_{\ell,n} = 0, \forall t$.

3.2. PV systems

Random quantity $P_{\text{av},n}$ denotes the maximum renewable-based generation at node $n \in \mathcal{N}_R \subseteq \mathcal{N}$ – hereafter referred to as the available real power. Particularly, $P_{\text{av},n}$ coincide with the maximum power point at the AC side of the inverter. When renewable energy sources (RESs) operate at unity power factor and inject the available real power $P_{\text{av},n}$, a set of challenges related to power quality and reliability in distribution systems may emerge for sufficiently high levels of deployed RES capacity; i.e., overvoltages may be experienced when RES generation exceeds load [19]. Efforts to ensure reliable operation of existing distribution systems with increased behind-the-meter renewable generation are focus on the possibility of inverters providing reactive power compensation and/or

curtailing real power. To account for the ability of the RES inverters to adjust the output of real power, let $\alpha_n \in [0, 1]$ denote the fraction of available real power curtailed by RES-inverter n. If no PV system/inverter is at a particular node i, $P_{av,i} = \alpha_i = 0$. For convenience, define the vectors $\boldsymbol{\alpha} := [\alpha_1, \ldots, \alpha_N]^\mathsf{T}$ and $\mathbf{p}_{\text{av}} := [P_{\text{av},1}, \ldots, P_{\text{av},N}]^\mathsf{T}$ where $\alpha_n = 0$, $P_{\text{av},n} = 0$, and $Q_n = 0$ for $n \in \mathcal{N} \backslash \mathcal{N}_R$.

The available real power from solar is modeled as $\mathbf{p}_{\text{av}} = \bar{\mathbf{p}}_{\text{av}} + \boldsymbol{\delta}_{\text{av}}$, where $\bar{\mathbf{p}}_{\text{av}} \in \mathbb{R}^N$ is a vector of the forecasted values and $\boldsymbol{\delta}_{\text{av}} \in \mathcal{R}_{\text{av}} \subseteq \mathbb{R}^N$ is a random vector whose distribution captures spatial dependencies among forecasting errors. We assume that the distribution system operator has a certain amount of information about the probability distributions of the forecasting errors $\boldsymbol{\delta}_{\text{av}}$. This information can come in the form of either knowledge of the probability density functions, or a model of $\boldsymbol{\delta}_{\text{av}}$ from which one can draw samples. In this paper, we make the assumption that these errors are Normally distributed; however, distributionally robust formulations of single chance constraints [20,13] can easily be incorporated into the framework here.

3.3. AC power flow approximation

Using (10), the net complex-power injections can be compactly written as

$$\mathbf{s} = \text{diag}(\mathbf{v})(\mathbf{Y}^*(\mathbf{v})^* + \bar{\mathbf{y}}^*(V_0)^*). \tag{11}$$

where $\mathbf{s} := [\mathbf{s}_1, \ldots, \mathbf{s}_N]^\mathsf{T}$, and $S_i = (1-\alpha_i)P_{av,i} - P_{l,i} - jQ_{l,i}$, $i \in \mathcal{N}$. This equation typically appears in the form of a constraint in standard OPF formulations, and introduces nonconvexities [21]. To derive a convex reformulation of the chance constrained OPF, linear surrogates of (11) and voltage-regulation constraints will be utilized. Collect voltages $\{V_n\}_{n\in\mathcal{N}}$ in the vector $\mathbf{v} := [V_1, \ldots, V_N]^\mathsf{T} \in \mathbb{C}^N$ and their magnitudes $\{|V_n|\}_{n\in\mathcal{N}}$ in $\mathbf{v_a} := [|V_1|, \ldots, |V_N|]^\mathsf{T} \in \mathbb{R}^N$. The objective is to obtain approximate power-flow relations whereby voltages are *linearly* related to injected powers:

$$\mathbf{v} \approx \mathbf{H}\mathbf{p} + \mathbf{J}\mathbf{q} + \mathbf{c} \tag{12}$$

$$\mathbf{v_a} \approx \mathbf{R}\mathbf{p} + \mathbf{B}\mathbf{q} + \mathbf{a}, \tag{13}$$

where $\mathbf{p} := \Re\{\mathbf{s}\}$ and $\mathbf{q} := \Im\{\mathbf{s}\}$ [22]. Then, formerly nonconvex constraints $|V_i| \le V^{\max}$, $i \in \mathcal{N}$, can be approximated as $\mathbf{R}\mathbf{p} + \mathbf{B}\mathbf{q} + \mathbf{a} \le V^{\max}\mathbf{1}_N$, while (12) and (13) represents surrogates of (11). While a single-phase equivalent is used in this paper for simplicity of exposition, the above linearization is also valid for three-phase AC power flow models.

Next, consider linearizing the AC power-flow equation around a given voltage profile $\bar{\mathbf{v}} := [\bar{V}_1, \ldots, \bar{V}_N]^\mathsf{T}$ [22]. In the following, the voltages $\mathbf{v}$ satisfying the nonlinear power-balance equations (11) are expressed as $\mathbf{v} = \bar{\mathbf{v}} + \mathbf{e}$, where the entries of $\mathbf{e}$ capture deviations around the linearization points $\bar{\mathbf{v}}$. Define $\bar{\mathbf{v}}_a \in \mathbb{R}^N_+$ the magnitudes of voltages $\bar{\mathbf{v}}$, and let $\bar{\boldsymbol{\gamma}} \in \mathbb{R}^N$ and $\bar{\boldsymbol{\mu}} \in \mathbb{R}^N$ collect elements $\{\cos(\bar{\theta}_i)\}$ and $\{\sin(\bar{\theta}_i)\}$, respectively, where $\bar{\theta}_i$ is the angle of the nominal voltage $\bar{V}_i$. Expanding on (11), and discarding second-order terms such as $\text{diag}(\mathbf{e})\mathbf{Y}^*\mathbf{e}^*$, it turns out that (11) can be approximated as $\boldsymbol{\Gamma}\mathbf{e} + \boldsymbol{\Phi}\mathbf{e}^* = \mathbf{s} + \upsilon$, where $\boldsymbol{\Gamma} := \text{diag}(\mathbf{Y}^*\bar{\mathbf{v}}^* + \bar{\mathbf{y}}^*V_0^*)$, $\boldsymbol{\Phi} := \text{diag}(\bar{\mathbf{v}})\mathbf{Y}^*$, and $\boldsymbol{\upsilon} := -\text{diag}(\bar{\mathbf{v}})(\mathbf{Y}^*\bar{\mathbf{v}}^* + \bar{\mathbf{y}}^*V_0^*)$. Next, consider then the following choice of the nominal voltage $\bar{\mathbf{v}}$:

$$\bar{\mathbf{v}} = -\mathbf{Y}^{-1}\bar{\mathbf{y}}V_0. \tag{14}$$

Using (14), it follows that $\boldsymbol{\Gamma} = \mathbf{0}_{N\times N}$ and $\upsilon = \mathbf{0}_N$, and therefore one obtains the linearized power-flow expression $\text{diag}\left(\bar{\mathbf{v}}^*\right)\mathbf{Y}\mathbf{e} = \mathbf{s}^*$. Notice that matrix $\mathbf{Y}$ is diagonally dominant and irreducible [22]. Particularly, it is diagonally dominant by construction since $|y_{kk}| \ge \sum_{i\ne k}|y_{ki}|$ for all $i \in \mathcal{N}$; it is also irreducibly diagonally dominant if $|y_{0k}| > 0$ for any k. Then, a solution for $\mathbf{e}$ can be expressed as $\mathbf{e} = \mathbf{Y}^{-1}\text{diag}^{-1}(\bar{\mathbf{v}}^*)\mathbf{s}^*$. Further, define the matrices:

$$\bar{\mathbf{R}} = \mathbf{Z}_R\text{diag}(\bar{\boldsymbol{\gamma}})(\text{diag}(\bar{\mathbf{v}}_\mathbf{a}))^{-1} - \mathbf{Z}_I\text{diag}(\bar{\boldsymbol{\mu}})(\text{diag}(\bar{\mathbf{v}}_\mathbf{a}))^{-1} \tag{15a}$$

$$\bar{\mathbf{B}} = \mathbf{Z}_I\text{diag}(\bar{\boldsymbol{\gamma}})(\text{diag}(\bar{\mathbf{v}}_\mathbf{a}))^{-1} + \mathbf{Z}_R\text{diag}(\bar{\boldsymbol{\mu}})(\text{diag}(\bar{\mathbf{v}}_\mathbf{a}))^{-1} \tag{15b}$$

where $\mathbf{Z}_R := \Re\{\mathbf{Y}^{-1}\}$ and $\mathbf{Z}_I := \Im\{\mathbf{Y}^{-1}\}$, and setting $\mathbf{H} = \bar{\mathbf{R}} + j\bar{\mathbf{B}}$, $\mathbf{J} = \bar{\mathbf{B}} - j\bar{\mathbf{R}}$, and $\mathbf{c} = \bar{\mathbf{v}}$. If the entries of $\bar{\mathbf{v}}$ dominate those in $\mathbf{e}$, then $\bar{\mathbf{v}}_\mathbf{a} + \Re\{\mathbf{e}\}$ serves as a first-order approximation to the voltage magnitudes [22], and relationship (13) can be obtained by setting $\mathbf{R} = \bar{\mathbf{R}}$, $\mathbf{B} = \bar{\mathbf{B}}$, and $\mathbf{a} = \bar{\mathbf{v}}_a$. Eqs. (12) and (13) are now utilized to solve the relaxed joint chance constraint problem.

4. Chance constrained formulation

4.1. Optimization problem reformulation

The original, unrelaxed joint chance constraint optimization for voltage regulation in distribution systems shown below:

$$(\text{P0}) \min_{\mathbf{v_a},\boldsymbol{\alpha}} \mathbb{E}(f(\mathbf{v_a}, \boldsymbol{\alpha}, \mathbf{p}_\ell, \mathbf{q}_\ell)) \tag{16a}$$

$$\text{subject to} \quad \mathbf{v_a} = \mathbf{R}((\mathbf{I} - \text{diag}\{\boldsymbol{\alpha}\})\mathbf{p}_{\text{av}} - \mathbf{p}_\ell) - \mathbf{B}\mathbf{q}_\ell + \mathbf{a} \tag{16b}$$

$$\Pr\{v_{a,1} \le V_{\max}, \ldots, v_{a,n} \le V_{\max}\} \ge 1 - \epsilon \tag{16c}$$

$$0 \le \alpha_i \le 1 \tag{16d}$$

for all $i \in \mathcal{N}$, where $v_{a,k}$ denotes the kth element of $\mathbf{v_a}$. Constraint (16b) represents a surrogate for the power balance equation; constraint (16c) is the joint chance constraint that require every voltage magnitude in the grid to be within upper and lower limits with at least $1-\epsilon$ probability; and constraint (16d) limits the curtailment percentage from 0 to 100%. The cost function $f(\mathbf{v_a}, \boldsymbol{\alpha}, \mathbf{p}_\ell, \mathbf{q}_\ell)$ is convex and can consider a sum of penalties on curtailment, penalties on power drawn from the substation, penalties on voltage violations, etc.[1].

As derived in Section 2.2, the above optimization problem, which is in general nonconvex due to constraint (16c), can be rewritten as the following optimization problem with single chance constraints:

$$(\text{P1}) \min_{\mathbf{v_a},\boldsymbol{\alpha}} \mathbb{E}(f(\mathbf{v_a}, \boldsymbol{\alpha}, \mathbf{p}_\ell, \mathbf{q}_\ell)) \tag{17a}$$

$$\text{subject to} \quad \mathbf{v_a} = \mathbf{R}((\mathbf{I} - \text{diag}\{\boldsymbol{\alpha}\})\mathbf{p}_{\text{av}} - \mathbf{p}_\ell) - \mathbf{B}\mathbf{q}_\ell + \mathbf{a} \tag{17b}$$

$$\Pr\{v_{a,i} \le V_{\max}\} \ge 1 - \epsilon_i \tag{17c}$$

$$0 \le \alpha_i \le 1 \tag{17d}$$

for all $i \in \mathcal{N}$, and each ϵ_i is chosen such that (9) holds.

4.2. Analytical reformulation of single chance constraints

The constraints (17c) can be then reformulated as exact, tractable constraints [23], assuming $\epsilon \le 0.5$. Assuming the joint distribution of the random variables is a multivariate Gaussian with mean $\boldsymbol{\mu}$ and covariance matrix $\boldsymbol{\Sigma}$, define μ_i as the ith value in $\boldsymbol{\mu}$ and σ as the (i, i) entry in $\boldsymbol{\Sigma}$. Then, define the following function at each node $i \in \mathcal{N}$:

$$h(p_{av,i}) = \sum_j (R_{ij}[(1-\alpha_j)p_{av,j} - p_{\ell,j}]) - \sum_j (B_{ij}q_{l,j}) + a_i - V_{\max}$$

[1] A generalized formulation would also include lower voltage limits; for simplicity of exposition in the high-penetration PV case shown in this paper, only upper limits were considered.

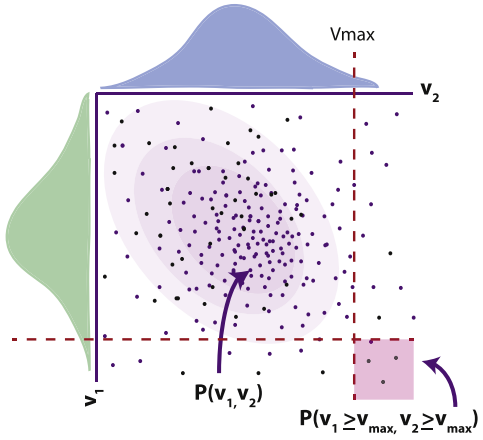

Fig. 2. Illustrative example with a joint multivariate normal distribution of voltage at two nodes and the region of interest; the probability of an overvoltage condition at both nodes.

where R_{ij} is the (i,j)th entry of $\mathbf{R}$, B_{ij} is the (i,j)th entry of $\mathbf{B}$, and a_i is the ith element of $\mathbf{a}$. Then $h(p_{av,i})$ is also Normally distributed with the following mean μ_i' and variance σ_i':

$$\mu_i' = \sum_j (R_{ij}[(1-\alpha_j)\mu_j - p_{\ell,j}]) - \sum_j (B_{ij} q_{l,j}) + a_i - V_{\max}$$
$$\sigma_i' = \sum_j R_{ij}(1-\alpha_j)\sigma_j$$

Thus, the constraints (17c) can be reformulated using the Gaussian cumulative distribution function (CDF) Φ:

$$\Pr\{h(p_{av,i}) \le 0\} = \Phi\left(\frac{0-\mu_i'}{\sigma_i'}\right) \ge 1-\epsilon_i$$

With the final analytical constraint written using the quantile function:

$$R_i[(1-\alpha_i)\mu_i - p_{\ell,i}] - B_i q_{\ell,i} + a_i - V_{\max} \le -R_i\alpha_i\sigma_i\Phi^{-1}(1-\epsilon_i) \quad (18)$$

Which can be explicitly included into problem (P1) for each node $i \in \mathcal{N}$ in place of constraints (17c).

4.3. Estimating the probability of intersection

Using a Monte-Carlo approach to reformulate the joint chance constraint into a series of deterministic ones can provide large computational burdens. According to [24], the number of realizations N_m of the uncertain parameter that need to be included as constraints in place of the chance constraint, with a β percent confidence level, should be at least the following:

$$N_m \ge \frac{2}{\epsilon}\left(\ln\left(\frac{1}{\beta}\right) + N_d\right) \quad (19)$$

where N_d is the total number of decision variables. For example, if $\epsilon = 0.01$, $N_d = 37$, and we desire with a 99% confidence level that the chance constraint will be fulfilled with probability $1-\epsilon$, 8,321 realizations of the random parameter is needed at each timestep. If we were to consider a model predictive control approach to the voltage regulation problem as in our previous work [4], a two-hour horizon with five minute timesteps, with 37 variables per timestep at these same confidence and violation levels would require $N_m \ge 178,521$ deterministic constraints at each receding horizon optimization. Here, we do not propose Monte-Carlo sampling for transforming the chance constraints into thousands of deterministic ones. Instead, we propose to tighten the bound used for each ϵ_i by estimating $P(A_1 \cap \cdots \cap A_n)$ through Monte-Carlo simulations.

An illustrative example of a joint multivariate normal distribution representing the distribution of voltage magnitude at two nodes is shown in Fig. 2, illustrating this region of interest. The proposed approach has the potential to be an improvement over Boole's, due to the fact that we can subtract this intersection from the sum of marginal probabilities, but if computational time is important, it is also an improvement over Monte-Carlo methods that estimate the joint chance constraint directly and require a large number of samples in order to accurately represent the original constraint. For each Monte-Carlo sample m generated from the joint multivariate normal distribution, we compute the intersection as follows:

$$P(A_1 \cap \cdots \cap A_n) \approx \frac{\sum_{m=1}^{N_m} \mathbf{1}_{\mathbf{v_a} \ge V_{\max}}(\mathbf{v_a}(m))}{N_m} \quad (20)$$

That is, for each sample that is drawn from the joint distribution of $\mathbf{p}_{av}$, the voltage magnitude is evaluated to see if V_{max} is violated. The policy for $\boldsymbol{\alpha}$ is utilized from the solution of that timestep where each $\epsilon_i = \epsilon/|\mathcal{N}_R|$, which is an upper bound for the new ϵ_i which will be updated after (20) is performed and calculated using (9). This is a fast calculation; for example, in the simulations in the following section, performing 10,000 calculations only required 0.19 s, and the resulting intersection probability calculated with 10,000 samples and with 100,000 samples only differed by.01%. In Fig. 3, a flowchart is shown of the overall process of converting the nonconvex joint chance constrained problem to the final convex optimization problem with single chance constraints.

5. Results and discussion

5.1. Results on IEEE-37 Node Test Feeder

The IEEE-37 node test feeder [25] was used for the following simulations. The actual five-minute load and solar irradiance data was obtained from [26] for the simulations, and shown in Fig. 4. In order to emulate a situation with high-PV penetration and risks

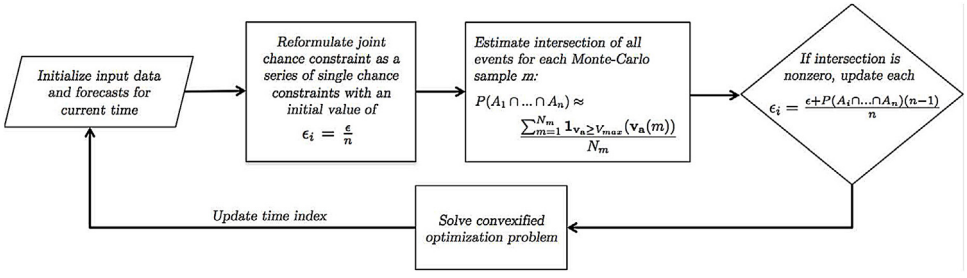

Fig. 3. Schematic of the proposed framework, illustrating the conversion of the nonconvex joint chance constrained problem to the final convex optimization problem.

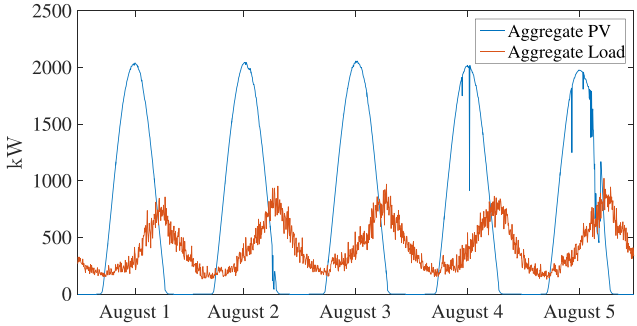

Fig. 4. Total feeder loading and available PV power during August 1–5, 2012.

of overvoltage, 16,200-kW rated PV systems were placed at nodes 3–18. We seek to minimize renewable curtailment; specifically,

$$f(\mathbf{v_a}, \boldsymbol{\alpha}, \mathbf{p}_\ell, \mathbf{q}_\ell) = \sum_{i \in \mathcal{N}} b_i \alpha_i^2, \tag{21}$$

where the cost of curtailing power at each node is set to be $b_i = \$0.10$. The number of samples was set to $N_m = 100,000$, which, as stated above, can be computed in a fraction of a second. The considered joint chance constraint maintains voltages at nodes $3 \cdots 37$, with the substation voltage at node 1 fixed to 1.03 p.u. Each μ_i, $i = 1, \ldots, n$ was chosen to be the power generated from the forecasted PV at that node, based on the aggregate solar irradiance from [26] and shifted using samples from a uniform distribution from ± 1 kW across each node. The covariance matrix Σ was formed by setting each entry (i, j) to $\Sigma_{ij} = \mathbf{E}[(P_{av,i} - \mu_i)(P_{av,j} - \mu_j)^T]$. Non-Gaussian probability distributions can also be considered in the proposed methodology by considering distributionally robust convex approximations of single chance constraints [3,4,20].

5.2. Comparison with deterministic and Boole's formulations

Simulations were performed using data from the first five days of August 2012, and using the joint chance constraint violation parameter $\epsilon = 0.01$.

5.2.1. Value of intersection term

During times of no solar irradiance, the observed probability of overvoltage is low; hence, the term $P(A_1 \cap \cdots \cap A_n)$ was not observed to be nonzero during these times. The value of this term can be seen Fig. 5 for August 1, 3, and 5; although the probability of intersection is rather small during peak solar irradiance hours, multiplying this term by $(n-1)$ results in a more significant value, reducing the conservativeness of Boole's inequality. Each ϵ_i in Boole's case was chosen to be $\epsilon_i = \frac{\epsilon}{n}$ [12,13]; and in the improved Boole's case, this parameter was set to $\epsilon_i = \frac{\epsilon + P(A_i \cap \cdots \cap A_n)(n-1)}{n}$, where $n = 16$ PV systems.

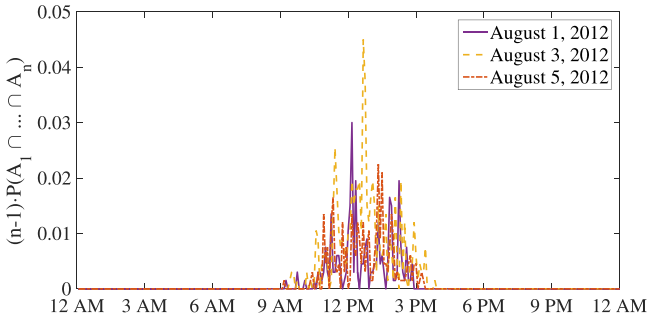

Fig. 5. Value of intersection term estimated from 100,000 Monte-Carlo samples.

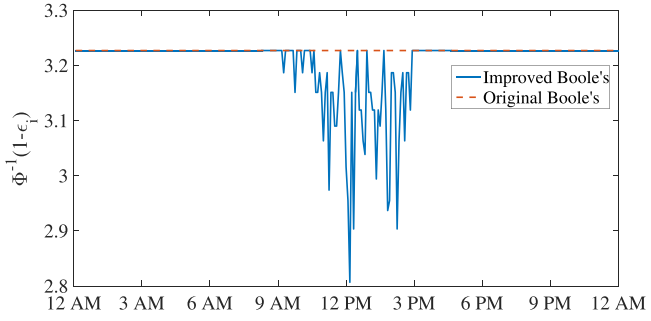

Fig. 6. The inverse CDF term for Aug. 1 under the original and improved Boole's inequality.

In Fig. 6, the value of each of the quantile functions $\Phi^{-1}(1-\epsilon_i)$'s is shown. By using Boole's inequality, the probability of constraint violation is held constant throughout the day, and is more conservative than the case where this parameter is calculated by using the improved Boole's inequality. When the improved inequality is used to calculate ϵ_i, the probability of violation is relaxed during times of solar irradiance. Because there is a nonzero probability of all considered voltages being too high, the conservative nature of Boole's inequality can be reduced by subtracting out the intersection of these events.

5.2.2. Cost vs. violation tradeoff

In order to validate the performance of the deterministic case (e.g., using the forecasted value for PV), the case where each ϵ_n was chosen according to Boole's inequality, and the case with the improved inequality, 10,000 Monte Carlo simulations were performed for August 1–5 for each of the methods. In Fig. 7, the total percentage of nodes with a voltage violation are shown for each of the three methods for August 1st. The deterministic case, which only considers the forecast of the PV (the mean of the random variables), violates the desired chance constraint bound of 0.01

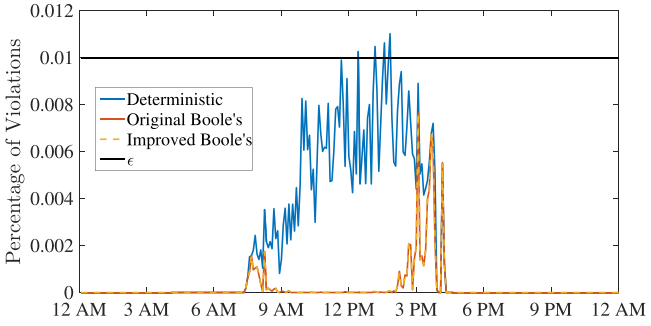

Fig. 7. Percentage of voltage violations for each Monte Carlo simulation during August 1.

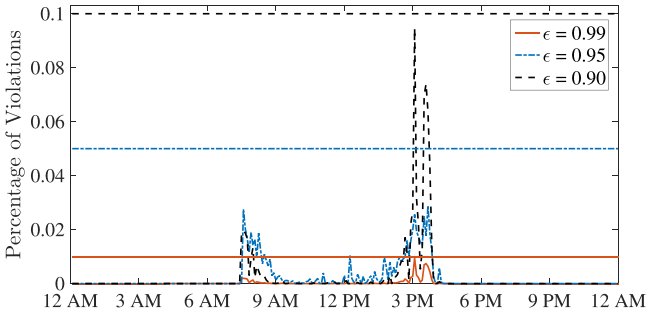

Fig. 8. Percentage of voltage violations for varying values of ϵ.

Table 1
Total cost of the three methods over the five-day simulation period.

Cost ($)	8/1	8/2	8/3	8/4	8/5	Total
Deterministic	18.03	15.56	13.76	13.99	11.76	73.10
Original Boole's	22.92	19.95	17.64	17.86	15.04	93.41
Improved Boole's	22.81	19.82	17.48	17.74	14.97	92.82

when compared with the chance constrained methods, because that method offers no guarantee that the voltages will be within limits with any probability. The difference between the number of voltage violations between the original Boole's method and the improved method are negligible; both bounds offer similar performance in terms of chance constraint violation probabilities. Fig. 8 illustrates the results for the same test day of August 1st, except with varying values of the chance constraint parameter ϵ. Clearly, as ϵ relaxes, the number of violations increases; however, as expected, the violations never exceed their maximum limit of $1-\epsilon$.

However, the benefit of the proposed method is demonstrated in terms of cost reduction. In Table 1, the total cost over the considered five-day simulation period for each of the method is shown. While the deterministic method results in the lowest cost, it also results in the highest number of violations, as well as offering little or no performance guarantee. The results from the optimization using the improved bound to calculate each ϵ_i result in a lower cost than that achieved by traditional Boole's, with a small additional computational cost.

6. Conclusion

In this paper, we presented a method for tractable computation of joint chance constraints in probabilistic AC OPF problems that improves upon Boole's inequality, which is often used to improve the tractability of joint chance constrained problems. The paper presented three main results: Firstly, a new application of joint chance constraints was applied to the distribution grid voltage regulation problem. Secondly, a computationally efficient technique for improving the traditional bound provided by Boole's inequality was developed. Lastly, the bound was validated analytically as well as experimentally, and the results showed an improvement in tightness over Boole's inequality.

An alternate tighter bound formed using Fréchet's inequality was also given for cases of large violation probabilities (for example, sensitivity studies where we wish to find the situations with high overvoltage probabilities). The improvement upon Boole's inequality hinges on the idea of subtracting the intersection of all considered events $n-1$ times, which is in general a very fast computation to make. The new bound was proven to be a valid upper bound, and in its worse case is equivalent to that of Boole's inequality. Simulation results presented here have shown that use of the new bound preserves the probabilistic guarantees of the original joint chance constraint, while reducing the cost and conservativeness of Boole's inequality. While Gaussian random variables were considered in this paper, the framework is not distribution-dependent and could also utilize a distributionally robust formulation for the resulting single chance constraints. Future work will consider sensitivity studies to first determine which nodes in the grid are susceptible to overvoltages, potentially increasing the impact of subtracting the intersection term. Efficient methods of calculating the other intersection/union terms due to the inclusion-exclusion principle that Boole's inequality unnecessarily includes will also be explored.

References

[1] L. Roald, F. Oldewurtel, T. Krause, G. Andersson, Analytical reformulation of security constrained optimal power flow with probabilistic constraints, in: IEEE PowerTech Conference, 2013.
[2] D. Bienstock, M. Chertkov, S. Harnett, Chance-constrained optimal power flow: risk-aware network control under uncertainty, SIAM Rev. 56 (3) (2014) 461–495.
[3] K. Baker, E. Dall'Anese, T. Summers, Distribution-agnostic stochastic optimal power flow for distribution grids, in: IEEE North American Power Symposium, Denver, CO, 2016.
[4] E. Dall'Anese, K. Baker, T. Summers, Chance-constrained ac optimal power flow for distribution systems with renewables, IEEE Trans. Power Syst. (2017).
[5] Q. Wang, Y. Guan, J. Wang, A chance-constrained two-stage stochastic program for unit commitment with uncertain wind power output, IEEE Trans. Power Syst. 27 (1) (2012) 206–215.
[6] M. Amini, A. Kargarian, O. Karabasoglu, Arima-based decoupled time series forecasting of electric vehicle charging demand for stochastic power system operation, Electric Power Syst. Res. 140 (2016) 378–390.
[7] H. Yu, C.Y. Chung, K.P. Wong, J.H. Zhang, A chance constrained transmission network expansion planning method with consideration of load and wind farm uncertainties, IEEE Trans. Power Syst. 24 (3) (2009) 1568–1576.
[8] K. Baker, G. Hug, X. Li, Energy storage sizing taking into account forecast uncertainties and receding horizon operation, IEEE Trans. Sustain. Energy 8 (1) (2017) 331–340.
[9] M. Vrakopoulou, K. Margellos, J. Lygeros, G. Andersson, Probabilistic guarantees for the $n-1$ security of systems with wind power generation, in: PMAPS 2012, 2012.
[10] M. Hojjat, M.H. Javidi, Chance-constrained programming approach to stochastic congestion management considering system uncertainties, IET Gen. Transm. Distrib. 9 (12) (2015) 1421–1429.
[11] G. Boole, An Investigation of the Laws of Thought on Which are Founded the Mathematical Theories of Logic and Probabilities (1854), Dover Publications, New York, NY, 1958.
[12] J.M. Grosso, C. Ocampo-Martinez, V. Puig, B. Joseph, Chance-constrained model predictive control for drinking water networks, J. Process Control 24 (5) (2014) 504–516.
[13] A. Nemirovski, A. Shapiro, Convex approximations of chance constrained programs, SIAM J. Optim. 17 (4) (2007) 969–996.
[14] L. Blackmore, M. Ono, Convex chance constrained predictive control without sampling, in: AIAA Guidance, Navigation and Control Conf., 2009.
[15] L. Hong, Y. Yang, L. Zhang, Sequential convex approximations to joint chance constrained programs: a Monte Carlo approach, IET Gen. Transm. Distrib. 59 (2011) 617–630.
[16] E. Erdoğan, G. Iyengar, Ambiguous chance constrained problems and robust optimization Mathematical Prog., vol. 107, 2006, pp. 37–61.
[17] G.A. Hanasusanto, V. Roitch, D. Kuhn, W. Wiesemann, Ambiguous Joint Chance Constraints Under Mean and Dispersion Information. Available at: http://www.optimization-online.org/DB_FILE/2015/11/5199.pdf.
[18] S. Zymler, D. Kuhn, B. Rustem, Distributionally robust joint chance constraints with second-order moment information, Math. Prog. 137 (1) (2013) 167–198.
[19] Y. Liu, J. Bebic, B. Kroposki, J. de Bedout, W. Ren, Distribution system voltage performance analysis for high-penetration PV, in: IEEE Energy 2030 Conf., 2008.
[20] T. Summers, J. Warrington, M. Morari, J. Lygeros, Stochastic optimal power flow based on conditional value at risk and distributional robustness, Int. J. Electric Power Energy Syst. 72 (2015) 116–125.
[21] J. Lavaei, S.H. Low, Zero duality gap in optimal power flow problem, IEEE Trans. Power Syst. 27 (1) (2012) 92–107.
[22] S. Dhople, S. Guggilam, Y. Chen, Linear approximations to AC power flow in rectangular coordinates, in: Allerton Conference on Communication, Control, and Computing, 2015.
[23] S. Boyd, L. Vandenberghe, Convex Optimization, Cambridge University Press, 2004.
[24] M.C. Campi, S. Garatti, M. Prandini, The scenario approach for systems and control design, Annu. Rev. Control 33 (1) (2009) 149–157.
[25] IEEE, 37 Node Distribution Test Feeder. Available at: https://ewh.ieee.org/soc/pes/dsacom/testfeeders/.
[26] J. Bank, J. Hambrick, Development of a High Resolution, Real Time, Distribution-Level Metering System and Associated Visualization Modeling, and Data Analysis Functions. Tech. Rep. NREL/TP-5500-56610, 2013, May.